Chapter 22

Protein Adsorption on Poly(ethylene oxide)-Grafted Silicon Surfaces

Susan J. Sofia and Edward W. Merrill

Department of Chemical Engineering, Massachusetts Institute of Technology, 77 Massachusetts Avenue, Room 56–291, Cambridge, MA 02139

Poly(ethylene oxide), in linear and star form, was covalently grafted to silicon surfaces in a range of grafting densities and the surfaces tested for their ability to adsorb proteins (cytochrome-c, albumin, fibronectin). The surfaces were analyzed by X-ray photoelectron spectroscopy (XPS) and ellipsometry, where both PEO content and amount of adsorbed protein were determined. All three proteins were found to reach zero adsorption at the highest grafting densities on all three linear PEG surfaces (PEG MW 3400, 10,000, and 20,000 g/mol). On both star PEO surfaces, albumin and fibronectin decreased to zero adsorption at intermediate grafting densities, whereas cytochrome-c continued to adsorb at all grafting densities. It was found that grafting densities of linear PEG in a brush regime were necessary to prevent protein adsorption. On PEO star surfaces, however, it was the decrease in space between grafted molecules to less than the size of the protein that was necessary in preventing the protein from adsorbing to the surface.

Increasing the biocompatibility of surfaces through the incorporation of PEO has been extensively investigated over the years. Two widespread ways of achieving this are: 1) by covalently binding of one or both ends of the PEO chain to an insoluble substrate surface, or 2) by incorporating PEO into a network with another polymer, either as an interpenetrating network (IPN) or covalently through a block copolymer network. Nagoaka and coworkers (*1,2*) end-linked one end of PEO via a methacrylate to various insoluble polymers. PEO end-linked at one or both ends, either to a surface or in a network, has been achieved with a wide variety of materials: segmented polyurethanes (where the PEO constitutes the "soft segment" continuous phase) (*3-8*), polysiloxanes (*9-11*) polystyrenes (*12-15*), polyfunctional isocyanates (*16*), poly(ethylene terephthalates) (*6,17*), poly(methyl methacrylates) (*6,18,19*), poly(lactic-glycolic acids) (*20*), poly(tetramethylene oxide) (*21*), and poly(vinyl chloride) (*22*). An important outcome of these studies is the common trend of decreasing protein and platelet adsorption and biological activity with increasing PEO

In Poly(ethylene glycol); Harris, J. Milton, et al.;
ACS Symposium Series; American Chemical Society: Washington, DC, 1997.

content, leading to the conclusion that the highest level of biocompatibility would be achieved when the surface consists solely of amorphous PEO polymer (*4,23*).

The accurate experimental characterization of PEO chains grafted to a polymer surface has traditionally been difficult to accomplish. This is mainly due to the fact that polymers can have very rough, non-uniform, and dynamic surfaces that make their accurate characterization quite a challenge. The use of X-ray photoelectron spectroscopy (XPS) or secondary ion mass spectrometry (SIMS) have traditionally been used, but these techniques primarily determine qualitatively the PEO content on the surface. The direct correlation of biological interactions with PEO surface content had not been achieved. At best, the efficacy of these surfaces was usually determined by observing the extent of biological interaction with them, and then correlating these interactions with the polymer characteristics, such as PEO molecular weight and PEO content in the material, but not specifically with the amount of PEO present on the surface.

There are several studies that have lent some insight into the PEO surface requirements needed for the prevention of protein adsorption. Prime et al. (*24*) studied protein adsorption onto surfaces containing PEG oligomers of varying content and molecular weight, which was achieved with self-assembled-monolayers (SAMs) on gold substrates (*24,25*). (We use PEG in place of PEO to refer to molecular weights of less than 25,000 g/mol.) The study showed convincingly that only very short lengths of PEO (PEGs of only 2 to 6 monomer units) can succeed, at sufficient densities, in preventing protein adsorption. This dispels the notion that very small molecular weight PEG loses its "ability" to repel proteins (*26*). Jeon et al. (*27,28*), in a theoretical study, modeled the protein resistance of a grafted PEO surface through a combination of hydrophobic interactions, Van der Waals attraction between a protein and the PEO/substrate surface, and steric repulsion of the grafted PEO chains as they are compressed by an approaching protein. The authors concluded that high surface densities and long chain lengths of PEO are desirable for resistance to protein adsorption, with surface density being the more important of the two parameters. However, the surface conditions considered by Jeon et al. were a dense, stretched-chain brush regime, which would be extremely difficult to achieve experimentally. It is generally found that the maximum grafting densities achieved from grafting solvated chains usually correlate to chain spacings on the order of the radius of gyration of the molecule (*29-32*). In addition, the authors state that certain assumptions and approximations that were made in their model lend the qualitative trends seen in their results to be valid, but the exact calculated values may not be entirely accurate. In the following experimental study, we hoped to achieve two things: first, to give a more realistic view of the dependence of protein adsorption on the surface content of grafted, randomly coiling PEO molecules, and second, to study protein adsorption on surfaces grafted with PEO star molecules, and compare the adsorption behavior with that found on linear PEO grafted surfaces.

PEO Grafted to Silicon Surfaces

Linear and star-shaped PEO molecules were grafted to silicon surfaces at varying grafting desities. In the case of the linear PEG surfaces, the range of grafting desities

spanned from a mushroom (individual chain) regime to the onset of a brush (overlapping, stretched chain) regime. Star surfaces consisted of individual star molecules grafted in increasing density up to the point of near chain overlap. Silicon wafers were used as a model substrate surface, where the surface is stable and extremely flat. A triaminosilane was covalently coupled to the surface, which provided a high concentration of grafting sites (both primary and secondary amines) for the attachment of the PEO (*33*). Tresyl chloride was used to couple the PEO hydroxyl chain ends to the amines on the surface (*34,35*), with a range of grafting densities being achieved by varying the concentration of tresylated PEO in the coupling solution (0.01 to 15 wt. %) (*36*).

Both linear and star-shaped PEO molecules were grafted to the silicon surfaces in order to study the differences in their grafting densities and effectiveness at preventing protein adsorption. Linear PEO random coils have a very loose, non-dense structure with only two chain ends per molecule. These chain ends could be located anywhere within the volume of the molecule, thus causing its grafting probability to decrease with increasing molecular weight. Their non-dense structure leads the chains to easily overlap with one another, even at low solution concentrations. PEG molecules of three molecular weights were grafted: 3400, 10,000, and 20,000 g/mol. Star molecules, on the other hand, having a central core region of poly(divinyl benzene) with PEO arms extending radially from that core (*37,38*), have a very dense, hard-sphere character which renders these molecules difficult to overlap except at extremely high concentrations (*39*). They have a large number of chain ends per molecule that are located at the outer regions of the molecule due to the steric hindrance within the core region (*40,41*). Thus, their probability of grafting to a surface is extremely high and would only decrease with a return to more random-coil characteristics (i.e., with increasing arm molecular weight or decreasing functionality). Two types of star molecules, reference numbers 228 and 3510, were bound to the silicon surface and have the following properties: #228: $\overline{Mw}$ = 200,000 g/mol, $\overline{M}_{arm}$ = 10,000 g/mol, $\bar{f}$ = 20; #3510,: $\overline{Mw}$ = 350,000 g/mol, $\overline{M}_{arm}$ = 5200 g/mol, $\bar{f}$ = 70 ($\bar{f}$ is the average number of arms per molecule, or its functionality).

The PEO surfaces were contacted with protein solutions of cytochrome-c, albumin, and fibronectin for 24 hours and the respective adsorptions measured. These three proteins were chosen because they span a wide range of sizes, from 12 kD for cytochrome-c (spherical in shape, diameter 34Å), 68 kD for albumin (spherical in shape, diameter 72Å), to 500 kD for fibronectin (rod-like shape, 600Å long and 25Å wide). This was so adsorption as a function of protein size could also be studied.

Analysis of the surfaces was performed using ellipsometry and X-ray photoelectron spectroscopy (XPS). This included a new method for measuring protein adsorption using XPS by measuring the attenuation of the underlying silicon signal and calculating the thickness of the adsorbed protein layer.

Analysis of PEO Surfaces

Thickness of Dried PEO Layer. XPS high resolution scans of the carbon 1s photoelectron were used to quantify the presence of the PEO on the surface using an aminosilane surface as a reference. Figure 1 shows an example of a high resolution

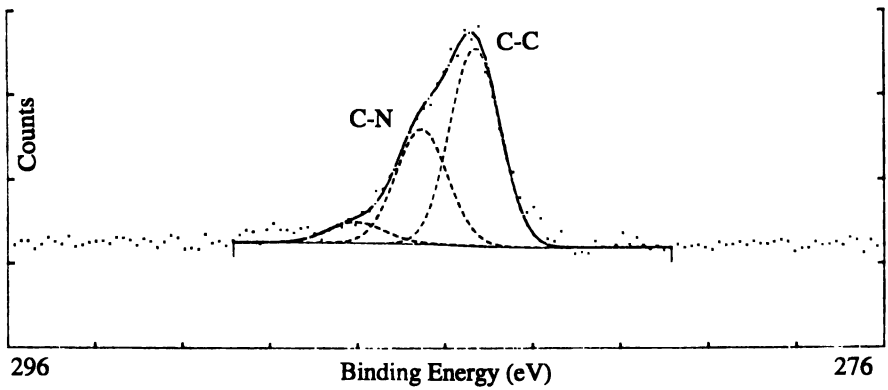

Figure 1. High resolution carbon scan of an aminosilane-coupled silicon surface.

carbon scan for an aminosilane control surface. The largest peak at lowest binding energy is indicative of alkane carbon (C-C), and the smaller, intermediate peak is the amine peak (C-N). The small, highest energy peak is probably due to the presence of carbon dioxide complexed onto the surface. Figures 2 and 3 show the scans for linear PEG 20k and star 3510 coupled surfaces at two different coupling concentrations of tresylated PEO. These scans clearly show the growing intensity of the ether peak of PEO (C-O, shifted 1.5 eV from the C-C peak) as the coupling concentration increases, indicating the increasing PEO content on the surface. It is important to remember that it is the dried (dehydrated) PEO layer that is being analyzed in XPS and ellipsometry, where any inhomogeneities on the surface are averaged out as if the surface had a uniform layer.

The intensity of the ether peak can be used to estimate the dried thickness of the PEO layer through the relation:

$$\frac{I}{I_o} = 1 - \exp\left(\frac{-d}{\lambda \sin(\theta)}\right) \quad (1)$$

where I is the intensity of the ether peak from a certain PEO layer thickness,
I_0 is the intensity from an "infinitely" thick PEO layer,
d is the thickness of the PEO layer (Å),
λ is the attenuation length of carbon 1s photoelectron through an organic layer (Å), and
θ is the take-off-angle used when taking the XPS measurements.

The attenuation length λ was found using the results of Laibinis et al. (*42*). Knowing θ and λ, and measuring I and I_o, values of the PEO thickness were calculated. These thicknesses were confirmed by ellipsometry, and PEO thickness as a function of tresylated PEO coupling concentration is shown in Figure 4.

Calculation of PEO Grafting Density. The values of the dry thickness of PEO were used to calculate the grafting density, σ , of the PEO molecules on the surface. The definition of grafting density for linear molecules is defined to be (*43*)

$$\sigma(\text{linear}) = \left(\frac{a}{L}\right)^2 \quad (2)$$

where a is the size of a monomer unit ($a \approx 3$ Å) (*24,27*), and L is the average distance between grafted, hydrated chains on the surface. The parameter L can be estimated from knowing the molecular weight, M, and the dry, grafted thickness, h, of PEO on the surface

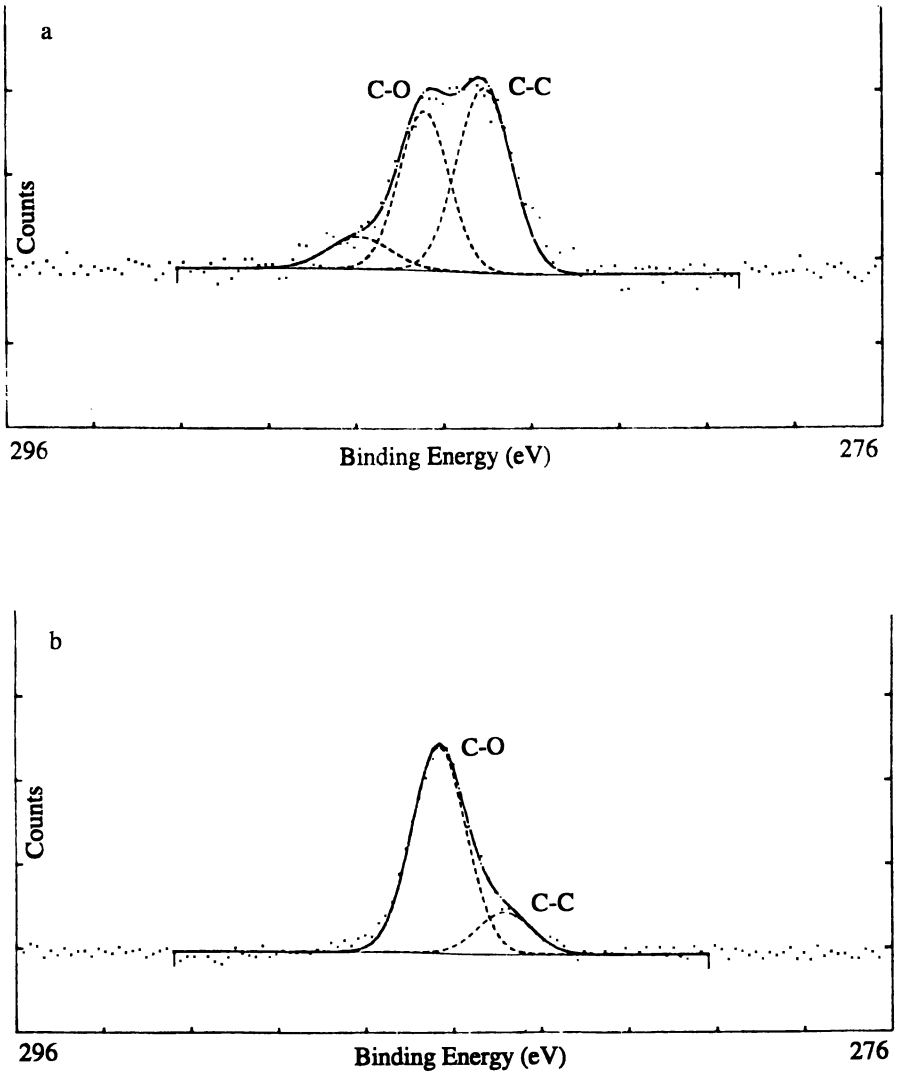

Figure 2. High resolution carbon scans of PEG 20k grafted surfaces from two different coupling concentrations (w/v): (a) 0.5%, (b) 15%.

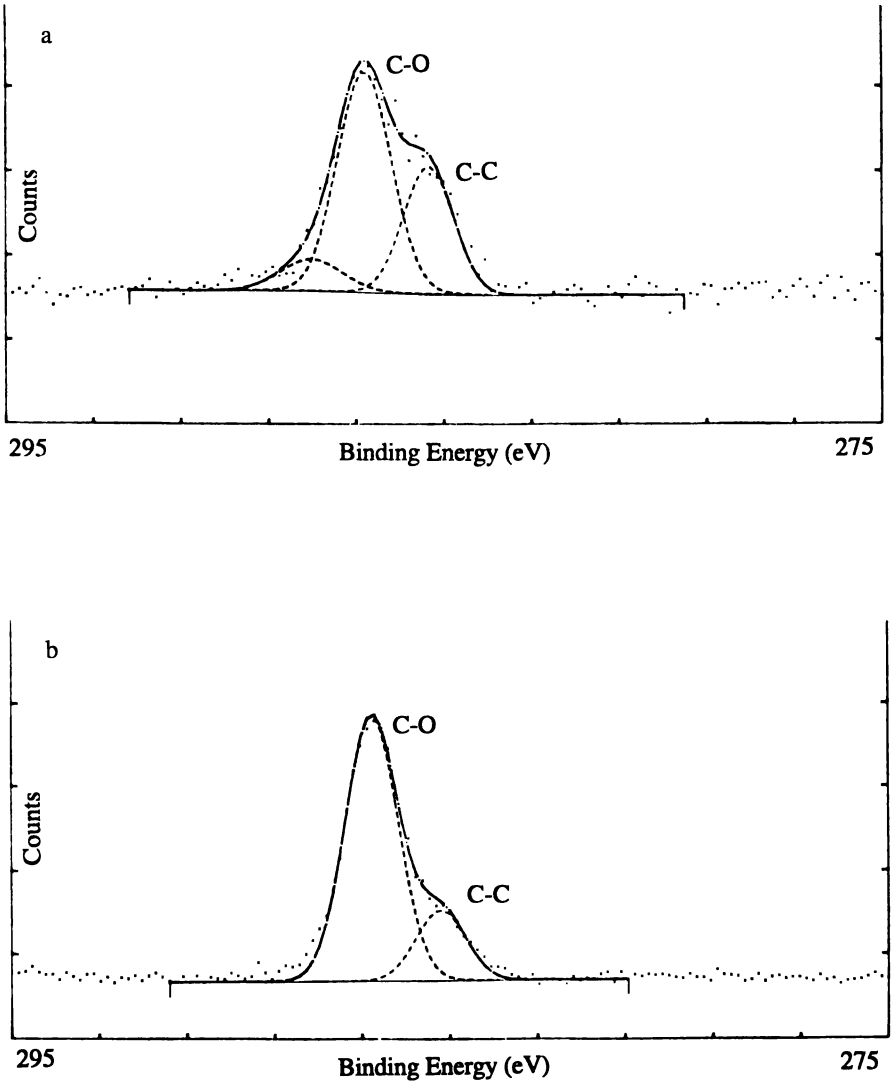

Figure 3. High resolution carbon scans of star 3510 grafted surfaces from two different coupling concentrations (w/v): (a) 0.05%, (b) 12%.

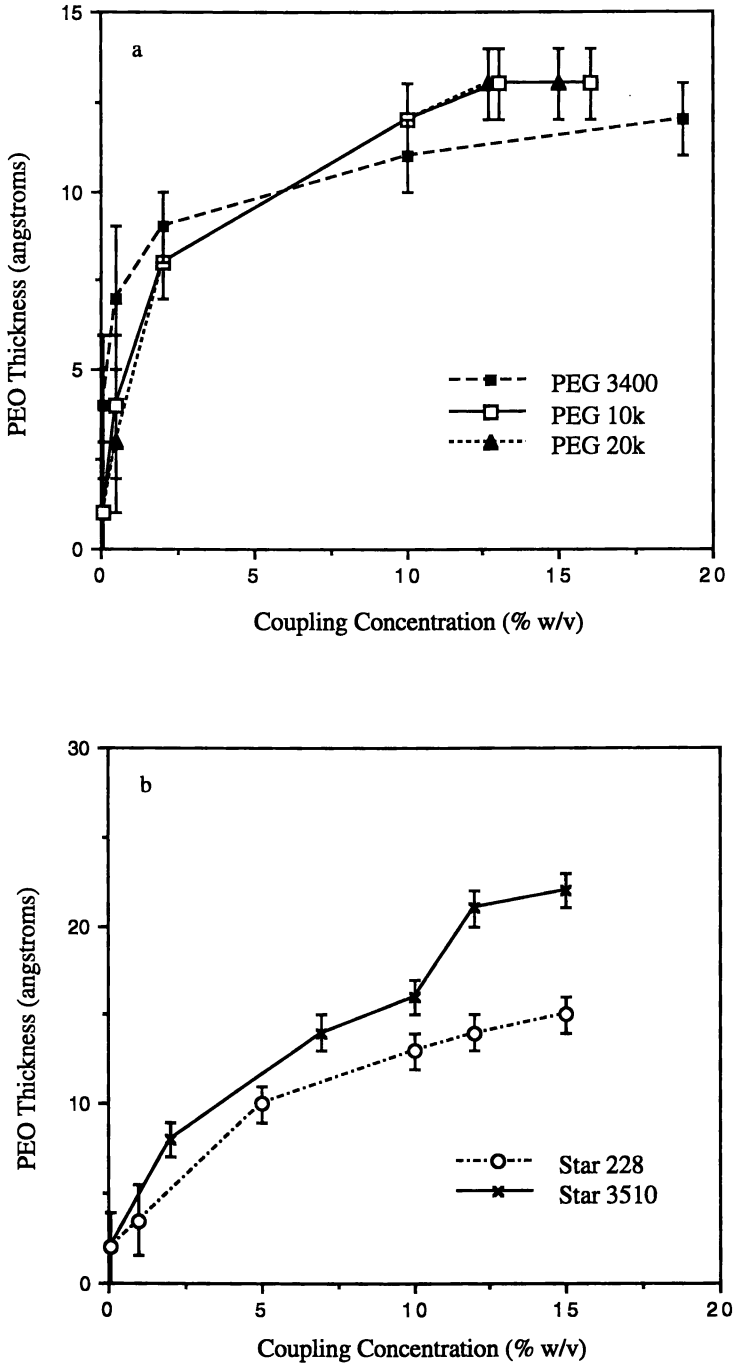

Figure 4. Dry PEO thickness as a function of tresylated PEO coupling concentration for: (a) linear PEG, and (b) star PEO.

$$L(\text{Å}) = \left(\frac{M}{\rho_{dry}\, h\, N_A} \right)^{1/2} \quad (3)$$

where ρ_{dry} is the density of the dry PEG layer and N_A is Avogadro's number.

Due to the large structural difference between linear and star PEO molecules, the size of a monomer unit is not appropriate to use in the calculation of grafting density for stars. Therefore, in place of a in equation 2, we use the radius of gyration, R_G^{star}, of the star molecules, since radius of gyration is a convenient parameter that can be measured or obtained (*39*). Grafting density for a star PEO surface is then

$$\sigma\,(\text{star}) = \left(\frac{R_G{}^{star}}{L} \right)^2 \quad (4)$$

PEO Chain Overlap. The relationship between attained grafting density and tresylated PEO coupling concentration for the three linear PEG molecules is shown in Figure 5. All three PEG molecules show the same general behavior of a rapid rise in grafting density at low coupling concentrations, with a leveling off such that a maximum grafting density is attained. This asymptotic behavior has been observed previously (*44,45*) and is mainly due to the interaction between grafted PEO chains on the surface. If we look at a calculation of the critical concentration of PEO, c_{crit}, marking the onset of chain overlap in solution, it can be estimated by

$$c_{crit} = \left(\frac{M}{N_A \frac{4}{3}\pi R_G{}^3} \right) \quad (5)$$

where R_G is the radius of gyration of the PEO molecule. For linear PEO molecules, this can be calculated from Flory (*46*); for stars it can be estimated from the results of Bauer et al. (*39*) or measured from light scattering experiments. Therefore, the critical concentrations for the three linear PEG solutions are $c_{crit}(3400) \approx 8$ %, $c_{crit}(10k) \approx 5$ %, and $c_{crit}(20k) \approx 3$ % (w/v). The highest coupling concentrations used in the experiments were 2.5 to 5 times larger than these c_{crit} values, indicating there was significant chain overlap in solution. The concentration of PEO at the surface is not necessarily the same as that in the bulk solution, but it is likely that significant chain overlap on the surface was also achieved. It is evident, therefore, that the surface becomes saturated in PEO such that steric hindrance and excluded volume effects have a strong influence on the chains binding to the surface, as expected. There is an increased resistance for additional PEO chains to penetrate the PEO layer and bind to the surface (*47*).

Figure 6 shows the attained grafting density as a function of tresyl-star coupling concentration for both star 228 and star 3510. Unlike the behavior of linear PEO, there

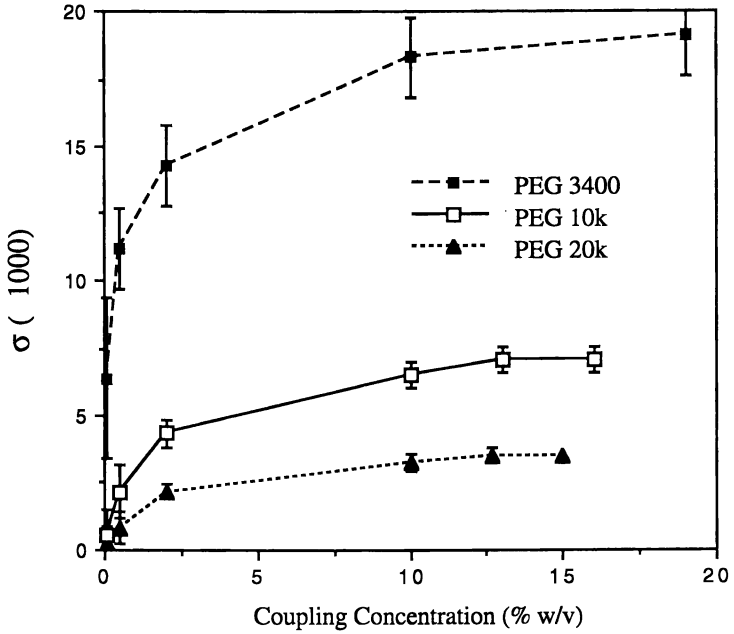

Figure 5. Grafting density as a function of tresylated PEO coupling concentration for linear PEG 3400, 10k, and 20k.

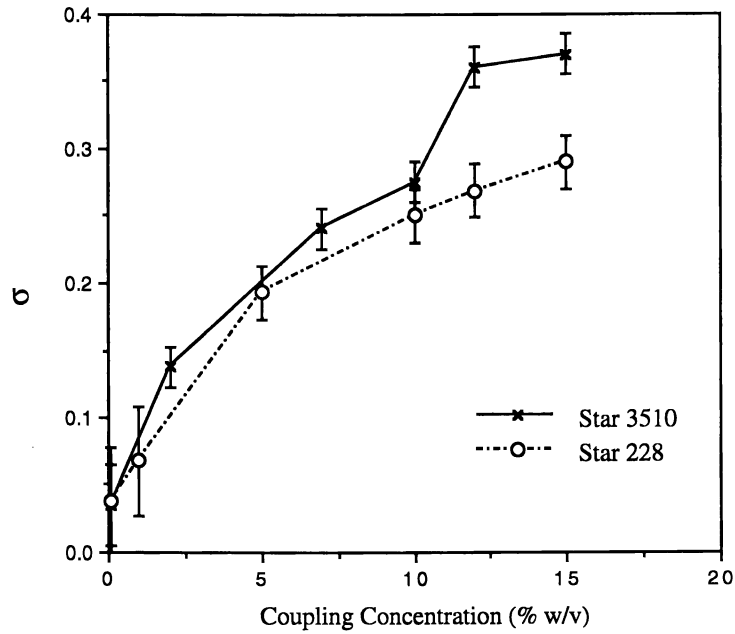

Figure 6. Grafting density as a function of tresylated PEO coupling concentration for stars 228 and 3510.

is no leveling off at a maximum grafting density at large concentrations. Instead, σ continues to increase even at the highest coupling concentrations. Again, we can explain these results by looking at the critical concentration of the molecules in solution: $c_{crit}(228) \approx 15\%$ and $c_{crit}(3510) \approx 13.5\%$. At the highest coupling concentration of 15%, both stars have just reached the point of overlap in solution. Therefore, from this point onward is where we would expect grafting density to reach a maximum due to steric repulsion and excluded volume effects on the surface. The extremely large values of c_{crit} for the stars are testimony to how dense the stars are, where such high concentrations are needed before the stars are forced to interpenetrate one another.

Protein Adsorption on PEO Surfaces

Measurement of Adsorbed Protein. The thickness of the layer of adsorbed protein can be determined by analyzing the attenuation of the silicon 2p photoelectron signal in an XPS scan, as referenced to the equivalent PEO surface not contacted with protein. The attenuation of a photoelectron signal due to an overlayer is described by the equation

$$\frac{I}{I_o} = \exp\left(\frac{-d}{\lambda \sin\theta}\right) \tag{6}$$

where I is the intensity of the Si 2p photoelectron with a protein overlayer,
I_o is the intensity of the Si 2p with no protein overlayer,
d is the thickness of the protein overlayer (Å),
λ is the attenuation length of Si 2p through an organic overlayer (Å), and
θ is the take-off-angle used in taking the measurements.

Therefore, the protein thickness, d, can be calculated by a measurement of I and I_0 in an XPS scan. This dry protein thickness can be converted to the common measure of adsorbed protein, ng/cm^2 or μg/cm^2, by estimating that the density of the adsorbed layer is ~1 g/cm^3. This is a safe assumption as, in general, most organic layers have a density close to 1 g/cm^3. In addition, proteins in aqueous solution have a fixed conformation such that they are not hydrated or swelled by water, and are therefore also thought to have a density close to 1 g/cm^3. Therefore, every Å thickness equals ca. 10 ng/cm^2 protein, with zero thickness being ≤ 1 ng/cm^2 of adsorbed protein.

Protein Adsorption on Linear PEG Surfaces. Figure 7 shows the adsorption as a function of PEO grafting density for cytochrome-c, albumin, and fibronectin on surfaces grafted with linear PEG 3400, 10k, and 20k, as measured by XPS. Again, these three proteins were chosen because they span a wide range of protein size, such that adsorption as a function of protein size could also be studied. At the lowest grafting densities where grafted PEO chains are sparse, there is maximum adsorption. As grafting density increases, the adsorption of all three proteins declines until it reaches zero adsorption at the highest grafting densities. This general behavior is the same on all three PEG surfaces. There are several important conclusions to draw from

these results. First, there is no specific PEO molecular weight, nor universal range of PEO grafting densities, that are necessary for the prevention of protein adsorption, at least in the ranges of protein size and PEG molecular weight studied. Rather, there is a defined minimum in grafting density for a given PEG molecular weight above which significant prevention of protein adsorption is achieved. This minimum correlates exactly with the onset of maximum achievable PEO grafting density (the "knee" of the curves) as shown in Figure 5. If we look more closely at the range of PEG grafting densities, we see that they span a range of PEG chain spacings of $L > R_G^{linear}$ to $L \leq R_G^{linear}$, i.e., from a mushroom to brush regime (*43*). Of significance is that it is at the transition point of $L \approx R_G^{linear}$, the onset of the brush regime, where the minimum in protein adsorption is reached. The brush region in good solvent is described as being when grafted chains repulse one another due to excluded volume and thus stretch away from the surface and from each other. This results in a more favorable enthalpic interaction of the polymer with the solvent (since $\chi < 0.5$) while sacrificing a loss of entropy due to the chains being more stretched (*30,48,49*). When a protein interacts with a PEO surface, it is rejected due to a steric repulsion force that is generated from the loss of configurational entropy as the PEO chains are compressed by the approaching protein (*27,31,50*). This repulsion force arises from a disruption of the PEO chain conformation and its interaction with surrounding water molecules. At high PEO segment densities, as in the brush regime, this repulsion force is then that much greater (*27*), and therefore we find that the proteins are rejected from the surface. The adsorption behavior seen with our PEG surfaces are in accordance with the findings of Malmsten and van Alstine (45), where PEO amphiphiles were adsorbed in varying densities to methylated silica and phosphatidic acid surfaces and the adsorption of several serum proteins was studied.

Another important finding from the above results is the fact that protein adsorption behavior on linear PEG surfaces seems to be independent of protein size, at least in the range of protein sizes studied, in that the adsorption of all three proteins decreases from maximum to minimum in the same range of grafting density for a given PEG surface. This can be explained through a comparison of the relative size of the proteins, d_p, compared to the size of the PEO chains, twice R_G. As found by Abbott et al. (*51-54*), the size of the protein relative to the PEO chain size has a significant effect on the partition coefficient of proteins in PEO/dextran two phase systems. If $d_p \ll 2R_G$, then the protein is small enough to enter the volume of the PEO chain with minimum disruption of the PEO chain, and the partition coefficient is increased. For $d_p \geq 2R_G$, the protein is excluded from the PEO chain volume and thus can only reside in the spacing between hydrated chains. When the PEO chains are overlapped in solution ($c > c_{crit}$), proteins become nearly completely excluded from the PEO rich phase, resulting in a significant decrease in the partition coefficient. The same phenomenon can be said to occur on PEO grafted surfaces, where we found that PEO overlap on the surface in a brush regime is very effective at preventing proteins ($d_p \geq 2R_G$) from reaching and adsorbing to the underlying surface. In addition, one recent theoretical study has evidenced that the kinetics of protein adsorption can be strongly influenced by not only PEO grafting density, but also on the molecular weight of the grafted PEO chains, in that grafted layers of higher molecular weight PEO, giving thicker PEO layers, can retard the rate of protein adsorption (*55*).

In Poly(ethylene glycol); Harris, J. Milton, et al.;
ACS Symposium Series; American Chemical Society: Washington, DC, 1997.

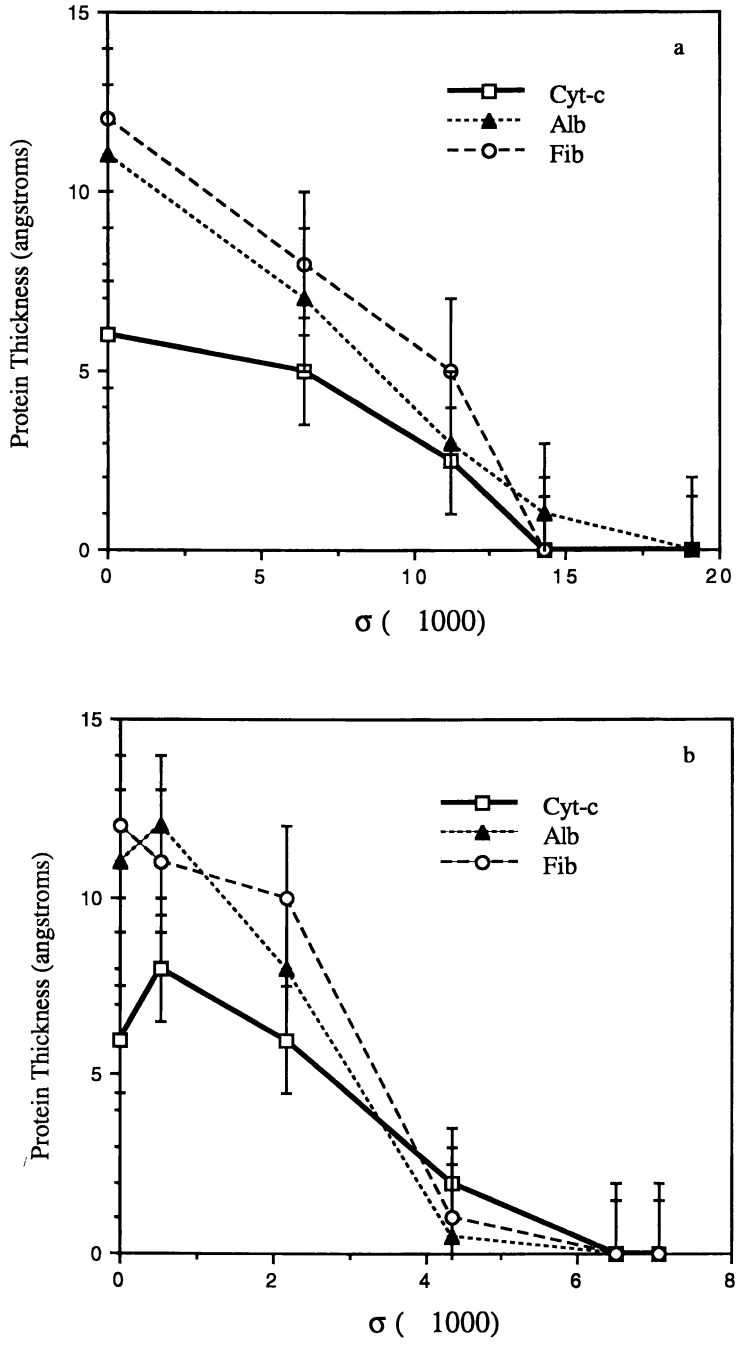

Figure 7. Protein adsorption as a function of linear PEG grafting density: (a) 3400, (b) 10k, and (c) 20k.

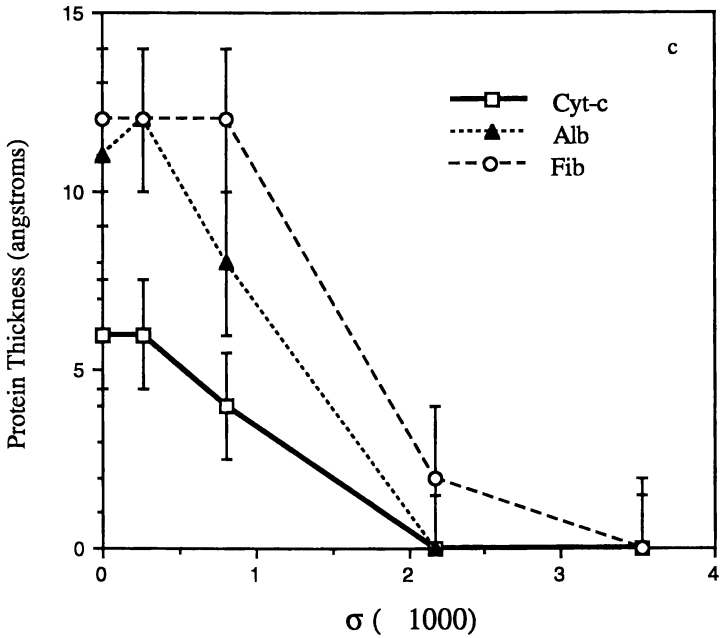

Figure 7. *Continued.*

The above findings are of particular significance when applied to the development of a polymer material having PEO grafted to or incorporated into its surface for the purpose of improving biocompatibility. In order to achieve sufficient PEO surface contents (i.e., a brush regime), the required grafting density increases as the molecular weight of the PEO decreases. In particular, for PEG molecular weights less than 1000-2000 g/mol, the required chain spacings would potentially need to be less than R_G to achieve a brush regime since they are no longer randomly coiling molecules, but rather have a more extended chain conformation when free in solution. This explains why in many of the studies cited in the beginning of this chapter, small PEO molecular weights and contents used in the polymer materials generally exhibited greater protein and platelet adsorption and thus poor enhancement in biocompatibility. Their surface content was too small (i.e., low grafting densities) to be very effective at preventing protein and platelet adsorption.

Protein Adsorption on Star PEO Surfaces. Figure 8 shows the protein adsorption of cytochrome-c, albumin, and fibronectin as a function of grafting density on each of the star PEO surfaces. Albumin and fibronectin show similar adsorption behavior, with a decline from maximum to minimum adsorption occurring in the range of low to intermediate star grafting densities. Cytochrome-c, in contrast, shows markedly different behavior. Rather than declining to zero adsorption, cytochrome-c continued to adsorb at all grafting densities, although with a decreasing trend. We can again look to the spacing of PEO chains to explain this behavior. The fact that the highest coupling concentrations used to bind the PEO stars to the surface was just at the point of chain overlap in solution leads us to conclude that there was also no overlap of star molecules on the surface. This then means that there are open spaces between grafted molecules on the surface. Star molecules are more dense in polymer segments than a linear molecule of equivalent hydrodynamic size, generally 2 to 3 times more dense or greater, as well as being almost melt-like in the core region of the molecule, leading stars to behave as hard spheres in solution. The steric repulsion force caused by an approaching protein would be tremendous, with little probability of a protein compressing or diffusing into a star molecule. Therefore, the only place for proteins to adsorb is in the spaces between star molecules. Protein size as it relates to the size of the open spaces on the surface thus plays a key role in adsorption. From the data shown in Figure 8, we can hypothesize that the grafting density of star molecules reached a point such that the open spaces became small enough to exclude albumin and fibronectin from the surface but not cytochrome-c. Taking into account the size of a hydrated star molecule, the average spacing between molecules on the surface, and the size of the protein, it was indeed found that albumin and fibronectin were excluded from the surface when the spaces between star molecules decreases to less than the size of the protein, but that cytocrhome-c remained smaller than these spaces even at the highest star grafting densities and thus continued to adsorb. Higher grafting densities resulting from higher coupling concentrations (forcing the star molecules into closer contact to overlap) would need to be achieved before the exclusion of small proteins like cytochrome-c could be realized. Overall, a surface fully covered with PEO star molecules has the potential to be much more effective than a linear PEO surface at

In Poly(ethylene glycol); Harris, J. Milton, et al.;
ACS Symposium Series; American Chemical Society: Washington, DC, 1997.

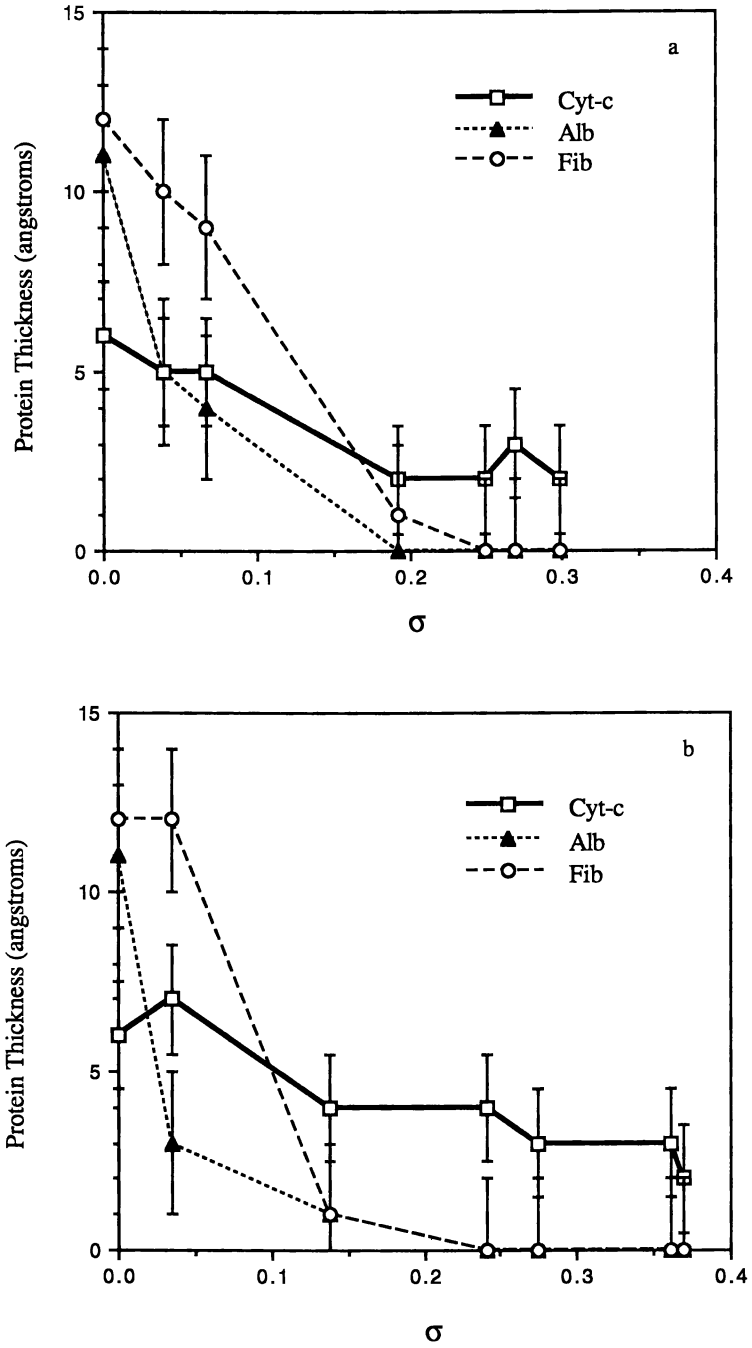

Figure 8. Protein adsorption as a function of PEO star grafting density: (a) star 228, and (b) star 3510.

preventing protein and cell adsorption, as star molecules, due to their hard-sphere character, are evidenced here to be essentially impenetrable by proteins.

Ellipsometry Results. The protein adsorption of the three proteins on each of the three PEG surfaces and two star surfaces were also measured by ellipsometry (data not shown). Due to the fact that the index of refraction of a protein layer, n_p, can vary by as much as ±25% depending on the specific protein that adsorbs, how much protein adsorbs, and possibly on the extent of denaturing, the results from ellipsometry can only be accepted for the general trend they reveal and not for the specific values of layer thickness measured (*24*). In this regard, the ellipsometry results correlated very well with the results obtained from XPS on all linear and star PEO surfaces.

Conclusions

In this chapter, we presented the key results from a study whose purpose was to investigate the dependence of protein adsorption on PEO surface content, molecular weight, PEO molecular type, and protein size. Silicon wafers provided a model surface on which accurate measurements with XPS and ellipsometry could be made.

The protein adsorption on the linear PEG surfaces was found to be independent of protein size, as $d_p \geq R_G^{linear}$. There was a decline from maximum to minimum adsorption of all three proteins in the same range of grafting density for a given PEG surface. What was found to be of main importance in the prevention of protein adsorption was the transition to a brush regime of the grafted PEO chains on the surface. Protein adsorption dropped to zero when chain spacings became smaller than R_G^{linear} (the chains being at least half-overlapped with each other). These findings are important in that they can be used as a guideline for the development of a material where increased biocompatibility through the grafting or incorporation of PEO into the surface is desired.

The protein adsorption behavior on star PEO surfaces was found to be markedly different than that on linear PEG surfaces. Adsorption on star surfaces is highly dependent on protein size. This is because star molecules are more dense in PEO than a linear molecule of equivalent hydrodynamic size such that they exhibit hard-sphere character in solution. Their dense structure results in the adsorption of proteins to occur only in the available spaces between grafted molecules, thus making the adsorption dependent on the relative sizes of the protein and the open spaces on the surface. Large coupling concentrations of PEO star molecules to greater than c_{crit} are needed to achieve overlap of PEO star molecules in solution as well as on the surface, so that a densely packed layer of star molecules on the surface can be realized.

Literature Cited

1. Mori, Y.; Nagoaka, S.; Takiuchi, H.; Kikuchi, T.; Noguchi, N.; Tanzawa, H.; Noishiki, Y. *Trans, Am. Soc. Artif. Internal Organs* **1982**, *28*, 459.
2. Nagoaka, S.; Mori, Y.; Takuchi, H.; Yokota, K.; Tanyawa, H.; Nishiumi, S. *Polymer Preprints* **1983**, *24*, 67.
3. Brash, J.L.; Uniyal, S. *J. Polym. Sci.* **1979**, *66*, 377.

4. Sa da Costa, V.; Brier-Russell, D.; Trudell, G.; Waugh, D.F.; Salzman, E.W.; Merrill, E.W. *J. Coll. Interface Sci.* **1980**, *76*, 594.
5. Mahmud, N.; Wan, S.; Sa da Costa, V.; Vitale, V.; Brier-Russell, D.; Kuchner, L.; Salzman, E.W.; Merrill., E.W. In *Physical Chemical Aspects of Polymer Surfaces*, Mittall, K.L., Ed., Plenum Press: New York, New York, 1983, Vol. 2.
6. Desai, N.P.; Hubbell, J.A. *Biomaterials* **1991**, *12*, 144.
7. Bots, J.G.F.; van der Does, L.; Bantjes, A. *Biomaterials* **1986**, *7*, 393.
8. Silver, J.H.; Myers, C.W.; Lim, F.; Cooper, S.L. *Biomaterials* **1994**, *15*, 695.
9. Verdon, S.L.; Chaikof, E.L.; Coleman, J.E.; Hayes, L.L.; Connolly, R.J.; Ramberg, K.; Merrill, E.W.; Callow, A.D. *Scanning Microscopy* **1990**, *4*, 341.
10. Chaikof, E.L.; Merrill, E.W.; Callow, A.D.; Connolly, R.J.; Verdon, S.L.; Ramberg, K. *J. Biomat. Mater. Res.* **1992**, *26*, 1163.
11. Sung, C.; Sobarzo, M.R.; Merrill, E.W. *Polymer* **1990**, *31*, 556.
12. Furusawa, K.; Shimura, Y.; Otobe, K.; Atsumi, K.; and Tsuda, K. *Kobanshi Ronbunshu* **1977**, *34*, 309.
13. Grainger, D.; Okano, T.; Kim, S.W. *Advances in Biomedical Polymers*, Plenum Press: New York, New York, 1987; pp. 229-247.
14. Bergstrom, K.; Holmberg, K.; Safrani, A.; Hoffman, A.S.; Edgell, M.J.; Kozlowski, A.; Hovanes, B.A.; Harris, J.M. *J. Biomat. Mater. Res.* **1992**, *26*, 779.
15. Bayer, E.; Rapp, W. In *Poly(Ethylene Glycol) Chemistry: Biotechnical and Biomedical Applications*; Harris, J.M., Ed.; Plenum Press: New York, New York, 1992; pp 325-344.
16. *Elastomers and Rubber Elasticity*; Mark J.E.; Lal, J., Eds.; ACS Symposium Series 193; American Chemical Society: Washington DC, 1982.
17. Desai, N.P.; Hubbell, J.A. *J. Biomed. Mater. Res.* **1991**, *25*, 829.
18. Shard, A.G.; Davies, M.C.; Tendler, S.J.B.; Nicholas, C.V.; Purbrick, M.D.; Watts, J.F. *Macromolecules* **1995**, *28*, 7855.
19. Drumheller, P.D.; Hubble, J.A. *J. Biomat. Mater. Res.* **1995**, *29*, 207.
20. Ferruti, P.; Penco, M.; D'Addato, P.; Ranucci, E.; Deghenghi, R. *Biomaterials* **1995**, *16*, 1423.
21. Ikeda, Y.; Kohjiya, S.; Takesako, S.; Yamashita, S. *Biomaterials* **1990**, *11*, 553.
22. Nagoaka, S.; Nakao, A. *Biomaterials* **1990**, *11*, 119.
23. Merrill, E.W.; Salzman, E.W. *Am. Soc. Artif. Intern. Organs* **1983**, *6*, 60.
24. Prime, K.L.; Whitesides, G.M. *J. Am. Chem. Soc.* **1993**, *15*, 10714.
25. Pale-Grosdemarge, C.; Simon, E.S.; Prime, K.L.; Whitesides, G.M. *J. Am. Chem. Soc.* **1991**, *113*, 12.
26. Osterberg, E.; Berstrom, K.; Holmberg, K.; Riggs, J.A.; Van Alstine, J.M.; Schuman, T.P.; Burns, N.L.; Harris, J.M. *Coll. Surf. A: Phys. Eng. Aspects* **1993**, *77*, 159.
27. Jeon, S.I.; Andrade, J.D.; deGennes, P.G. *J. Colloid Interface Sci* **1991**, *142*, 149.
28. Jeon, S.I.; Andrade, J.D. *J. Collard Interface Sci* **1991**, *142*, 159.
29. Auroy, P.; Auvray, L.; Léger, L. *Phys. Rev. Lett.* **1991**, *66*, 719.
30. Hommel, H.; Halli, A.; Touhami, A.; Legrand, A.P. *Colloids and Surfaces* **1996**, *111*, 67.

31. Gölander, C.-G.; Herron, J.N.; Lim, K.; Claesson, P.; Stenius, P.; Andrade, J.D. In *Poly(Ethylene Glycol) Chemistry: Biotechnical and Biomedical Applications;* Harris, J.M., Ed.; Plenum Press: New York, New York, 1992; pp 221-244.
32. Huang, S.-C.; Caldwell, K.D.; Lin, J.-N.; Wang, H.-K.; Herron, J.N. *Langmuir* **1996**, *12*, 4292.
33. Stenger, D.A.; George, J.H.; Dalcey, C.S.; Hickman, J.J.; Rudolph, A.S.; Nielsen, T.B.; McCort, S.M.; Calvert, J.M. *J. Am. Chem. Soc.* **1992**, *114*, 8435.
34. Nilsson, K.; and Mosback, K., *Biochem. Biophys. Res. Comm.*, **1981**, *102*, 449.
35. Nilsson, K., Mosback, K. *Methods Enzymology* **1984**, *104*, 56.
36. Sofia-Allgor, S.J., PhD. Thesis, Massachusetts Institute of Technology, 1996.
37. Gnanou, Y.; Lutz, P.; Rempp, P. *Makromol. Chem.* **1988**, *189*, 2885.
38. Lutz, P.; Rempp, P. *Makromol. Chem.* **1988**, *189*, 1051.
39. Bauer, B.J.; Fetter, L.J.; Graessley, W.W.; Hadjichristidis, N.; Quack, G. *Macromolecules* **1989**, *22*, 2337.
40. Daoud, M.; Cotton, J.P. *J. Phys.* (Paris, Fr.) **1982**, *43*, 531.
41. Douglas, J.F.; Roovers, J.; Freed, K.F. *Macromolecules* **1990**, *23*, 4168.
42. Laibinis, P.E.; Bain, C.D.; Whitesides, G.M. *J. Phys. Chem.* **1991**, *95*, 7017.
43. DeGennes, P.G. *Macromolecules* **1980**, *13*, 1069.
44. Herder, P.C.; Claesson, P.M.; Herder, C.E. *J. Colloid Interface Sci.* **1988**, *119*, 240.
45. Malmsten, M.; val Alstine, J.M. *J. Colloid Interface Sci.* **1996**, *177*, 502.
46. Flory, P. *Principles of Polymer Chemistry*; Cornell University Press: Ithaca, NY, 1953.
47. Kopf, A.; Baschnagel, J.; Wittmer, J.; Binder, K. *Macromolecules* **1996**, *29*, 1433.
48. Carignano, M.A.; Szleifer, I. *Macromolecules* **1995**, *28*, 3197.
49. Milner, S.T. *Science* **1991**, *251*, 905.
50. Antonsen, K.P.; Hoffman, A.S. In *Poly(Ethylene Glycol) Chemistry: Biotechnical and Biomedical Applications;* Harris, J.M., Ed.; Plenum Press: New York, New York, 1992; pp 15-27.
51. Abbott, N.L.; Blankschtein, D.; Hatton, T.A. *Macromolecules* **1991**, *24*, 4334.
52. Abbott, N.L.; Blankschtein, D.; Hatton, T.A. *Macromolecules* **1992**, *25*, 3917.
53. Abbott, N.L.; Blankschtein, D.; Hatton, T.A. *Macromolecules* **1992**, *25*, 3932.
54. Abbott, N.L.; Blankschtein, D.; Hatton, T.A. *Macromolecules* **1992**, *25*, 5192.
55. Szleifer, I. *Biophysical J.* **1997**, *72*, 595.